Supporting Information

Coaxial Yarn Electrode Based on Hierarchical MoS$_2$ Nanosheets/Carbon Fiber Tows for Flexible Solid-State Supercapacitors

Lili Gao[*a], Xuelian Li[a], Xiaodong Li[b], Jianli Cheng[b], Bin Wang[b], Zhiyu Wang[a], Changming Li[c]

[a] College of Environmental Science & Engineering, Taiyuan University of Technology, Taiyuan 030024, Shanxi, Peoples R China

[b] Institute of Chemical Materials, China Academy of Engineering Physics, Mianyang 621900, Sichuan, Peoples R China

[c] Institute of Clean Energy & Advance Material, Southwest University, Chongqing 400715, Peoples R China

Synthesis of MoS$_2$ NSs

Typically, $(NH_4)_6Mo_7O_{24} \cdot 4H_2O$ (0.14 mmol) and CH_4N_2S (2.00 mmol) were respectively dissolved in deionized water under vigorous stirring to form a homogeneous solution. The reaction was conducted at 200 °C for 9 h in an electric oven. After reaction, the samples were cooled to room temperature naturally, washed several times with deionized water and absolute ethanol, and then dried at 80 °C for 6 h under vacuum.

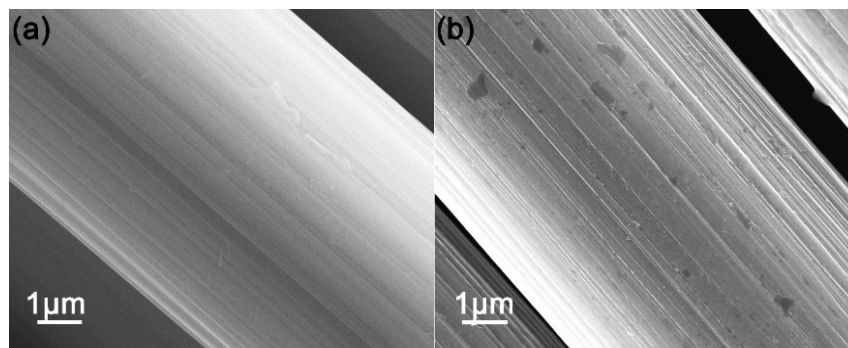## Supporting Figures and some illustrations

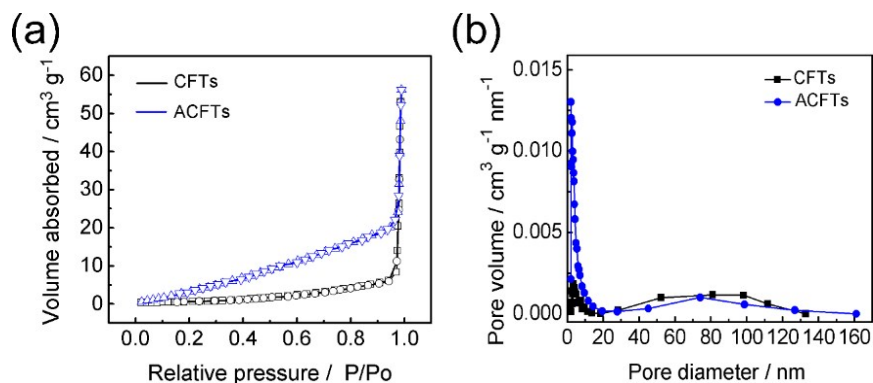**Figure S1.** SEM images of a single CF (a) and ACF (b).

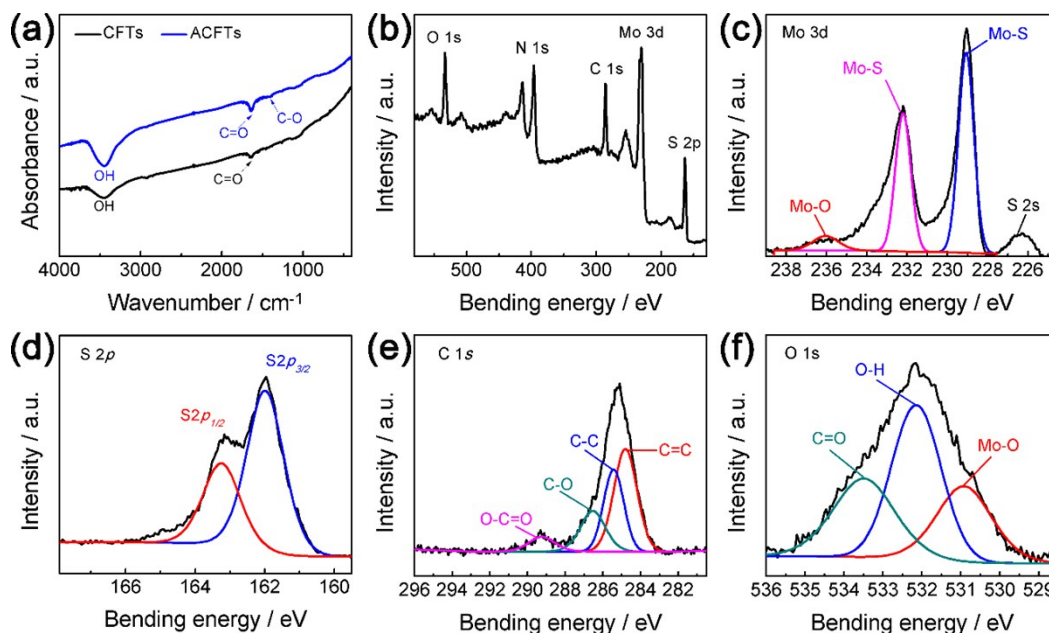**Figure S2.** Nitrogen adsorption/desorption isotherms (a) and pore-size distribution (b) of CFTs and ACFTs.

Figure S3. (a) The FTIR spectra of CFTs and ACFTs; (b) Low resolution XPS spectrum of ACFTs/MoS$_2$; High resolution XPS spectrum of Mo 3d (c), S 2p (d), C 1s (e) and O 1s (f) of ACFTs/MoS$_2$.

(1) Illustration for XPS spectra in figures S3b-S3f

The oxidation state and chemical composition of the ACFTs/MoS$_2$ were analyzed by XPS. Wide scan XPS spectra of ACFTs/MoS$_2$ is shown in Figure S3b. Carbon (C), nitrogen (N), sulfur (S) and molybdenum (Mo) peaks can be observed, in which N element may come from nitrogen-contained precursor in the solution of ((NH4)$_2$S$_2$O$_8$).[1] As seen in Figure S3c, there are two characteristic peaks at 229.1 and 232.2 eV, which correspond to the Mo 3d$_{5/2}$ and Mo 3d$_{3/2}$ orbitals, respectively, suggesting a Mo (IV) characteristic in MoS$_2$. The peak at 236.1 eV related to the Mo 3d$_{5/2}$ corresponding to Mo (VI) is in agreement with typical Mo-O bonds,[2] while the

peak at 226.0 eV can be indexed as S2s. The binding energies located at 162.0 and 163.3 eV are due to S $2p_{3/2}$ and $2p_{1/2}$ of MoS_2, respectively (Figure S3d). Above binding energy are all in good agreement with values of MoS_2 crystal reported previously.[3] The C1s XPS profile of the $ACFTs/MoS_2$ (Figure S3e) showed two main strong peaks, corresponding to the sp^2 C=C and C-C bonds at 284.8 and 286.5 eV. In general, the C1s spectrum of ACFTs showed another two peaks centered at 286.5 and 289.2 eV, which correspond to the binding energy of C-O bonds and O–C=O bonds, respectively.[4-7] Therefore, the C1s spectrum of the $ACFTs/MoS_2$ indicates the oxidation of ACFTs (with oxygen containing functionalized groups). Figure S3f shows the narrow XPS spectrum of O 1s, in which three peaks can be found in the case of $ACFTs/MoS_2$, with one peak around 531.0 eV relating to the Mo-O bonds and another two peaks around 532.2 and 533.5 eV corresponding to O–H bonds and C=O bonds, respectively. The O 1s peak around 531.0 eV cannot be associated with MoO_3 phase whose peak is expected at 530.6 eV.[8] The O–H bonds and C=O bonds found in spectrum of O 1s further confirm that the acid treatment can introduce oxygen-containing groups on the surface of CFT. Meanwhile, the weak Mo-O bonds (531.0 eV) and Mo-O bonds (236.1 eV) seen in XPS spectrum of Mo 3d both indicate that the existence of oxygen element plays a critical role in connecting MoS_2 and carbon fiber through Mo-O-C chemical bond.
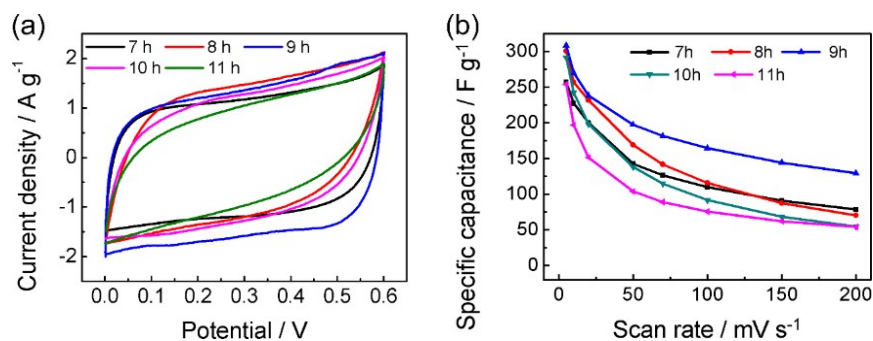

Figure S4. CV performance (a) and plots of specific capacitance *vs* scan rate (b) of $ACFTs/MoS_2$ electrode synthesized for different time
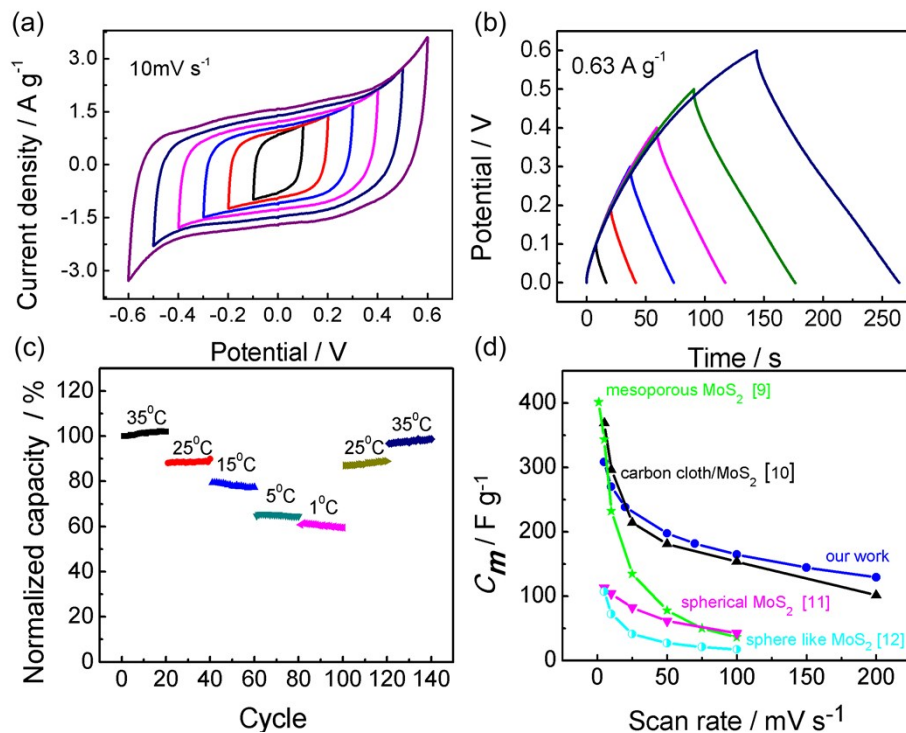
Figure S5 Electrochmical performances of ACFTs/MoS$_2$ planar pattern SC. (a) CV curves under different voltage windows at 10 mV s^{-1}; (b) GCD performances under different voltage ranges at 0.63 A g^{-1}; (c) Normalized Capacity under different controlling temperatures (c); (d) Comparison of mass specific capacitance of MoS$_2$-based SC in recent papers.[9-12]

(2) Illustration for temperature influence on capacitance in figures S5c

The influence of measuring temperature on the electrochemical performances of ACFTs/MoS$_2$ planar pattern SC is shown in Figure S5c. To get the results, the charging-discharging performance of ACFTs/MoS$_2$ planar pattern SC was measured at constant current density of 2.21 A g^{-1}, and the ambient temperature was controlled to decrease from initial 35 ^{o}C to 1 ^{o}C and then recover to 35 ^{o}C, and under each temperature, only the SC was charged-discharged twenty times. All the capacities gained under different temperatures was normalized to the initial capacity under 35 ^{o}C, and then the normalized capacity could be got. As the temperature decreases from 35 ^{o}C to 1 ^{o}C, the capacity decreases gradually to 61.2% of its initial value with good stability at each test temperature and recovers to 98.7% of the initial value as the temperature increased to 35 ^{o}C, demonstrating that the ambient temperature has an impact on specific capacitance.

Calculation of electrochemical capacitance:

The specific capacitance of electrodes, including mass specific capacitance (C_m) and volumetric specific capacitance (C_v), are calculated according to formulas (1) and (2) reported previously [13], where C is the measured capacitance (from CV) in the two-electrode configuration, M and V are respectively the mass of MoS_2 nanosheets and volume of the single fiber electrode.

$$C_m = 2C/M \qquad (1)$$

$$C_v = 2C/V \qquad (2)$$

The mass energy density (E_m), volumetric energy density (E_v), mass power density (P_m) and volumetric power density (P_v) can be obtained according to formulas (3-6) from GCD curves, where t is the discharge time, U represents the potential window.

$$E_m = C_m \times U^2 \times 8^{-1} \times 3.6^{-1} \qquad (3)$$

$$E_v = C_v \times U^2 \times 8^{-1} \times 3.6^{-1} \qquad (4)$$

$$P_m = E_m \times 3,600 \times t^{-1} \qquad (5)$$

$$P_v = E_m \times 3,600 \times t^{-1} \qquad (6)$$

Supporting References:

1. Y. Zhao, L. Kuai, Y. Liu, P. Wang, H. Arandiyan, S. Cao, J. Zhang, F. Li, Q. Wang, B. Geng and H. Sun, *Scientific Reports*, 2015, **5**, 8722.

2. E. G. da Silveira Firmiano, A. C. Rabelo, C. J. Dalmaschio, A. N. Pinheiro, E. C. Pereira, W. H. Schreiner and E. R. Leite, *Advanced Energy Materials*, 2014, **4**, 175-178.

3. J. Zhou, J. Qin, X. Zhang, C. Shi, E. Liu, J. Li, N. Zhao and C. He, *ACS Nano*, 2015, **9**, 3837-3848.

4. H. Yang, Y. Lu, K. Lin, S. Hsu, C. Huang, S. She, H. Liu, C. Lin, M. Xiao, S. Wey, P. Chen, T. Yen, K. Wei and C. Ma, *Biomaterials*, 2013, **34**, 7204-7214.

5. K. Krishnamoorthy, M. Veerapandian, R. Mohan and S. Kim, *Appl. Phys. A*, 2012, **106**, 501-506.

6. A. Van Deynse, P. Cools, C. Leys, R. Morent and N. De Geyter, *Surface and Coatings Technology*, 2015, **276**, 384-390.

7. Y. Liu, X. Zhang, C. Song, Y. Zhang, Y. Fang, B. Yang and X. Wang, *Materials & Design*, 2015, **88**, 810-819.

8.   W. J. Dong, J. Ham, G. H. Jung, J. H. Son and J. L. Lee, *Journal of Materials Chemistry A*, 2016, **4**, 4755-4762.

9.   M. S. Javed, S. Dai, M. Wang, D. Guo, L. Chen, X. Wang, C. Hu and Y. Xi, *Journal of Power Sources*, 2015, **285**, 63-69.

10.   A. Ramadoss, T. Kim, G.-S. Kim and S. J. Kim, *New Journal of Chemistry*, 2014, **38**, 2379-2385.

11.   P. Ilanchezhiyan, G. M. Kumar and T. W. Kang, *Journal of Alloys & Compounds*, 2015, **634**, 104-108.

12.   K. Krishnamoorthy, G. K. Veerasubramani, S. Radhakrishnan and J. K. Sang, *Materials Research Bulletin*, 2013, **50**, 499-502.

13.   L. Liu, Y. Yu, C. Yan, K. Li and Z. Zheng, *Nat Commun*, 2015, **6**, 7260.